Liquid Crystals
Publication details, including instructions for authors and subscription information:
http://www.informaworld.com/smpp/title~content=t713926090

A review of textures of the TGBA* phase under different anchoring geometries

I. Dierking

Online publication date: 06 August 2010

To cite this Article Dierking, I.(1999) 'A review of textures of the TGBA* phase under different anchoring geometries', Liquid Crystals, 26: 1, 83 — 95
To link to this Article: DOI: 10.1080/026782999205588
URL: http://dx.doi.org/10.1080/026782999205588

LIQUID CRYSTALS, 1999, VOL. 26, NO. 1, 83–95

A review of textures of the TGBA* phase under different anchoring geometries

I. DIERKING* and S. T. LAGERWALL

Department of Physics, Division of Microelectronics and Nanoscience, Chalmers University of Technology, S-41296 Göteborg, Sweden

(*Received 15 June 1998; accepted 26 August 1998*)

Polarizing microscope textures of the twist grain boundary A* (TGBA*) phase are reviewed for two different compounds in different geometries with different surface treatments giving monostable planar and homeotropic boundary conditions. The textures are discussed in the light of the helical structure of the TGBA* phase. Depending on the compound, the underlying phase is either SmA* or SmC*, whereas the adjacent phase at higher temperature is cholesteric (N*). Sample preparations in wedge-shaped cells subjected to a slight temperature gradient exhibit TGBA* textures much more typical for the cholesteric than for the ordinary SmA* phase. For instance, Grandjean steps and fingerprint textures are observed for planar and homeotropic boundary conditions, respectively. Preparation of smectic droplets clearly reveals the helical axis of the TGBA* phase to be perpendicular to the helical axis of the helielectric SmC* phase. For thin samples, a suppression of the TGBA* helix leading to a surface-induced structure corresponding to a conventional bulk SmA* phase is observed. Under certain conditions, a cholesteric phase in the vicinity of a twist inversion point may exhibit very similar textures to the TGBA* phase near the transition to the SmA* phase. On exemplified textures similarities are discussed and differences pointed out.

1. Introduction

Ten years ago a novel liquid crystal phase consisting of chiral molecules was theoretically predicted by Renn and Lubensky [1] on the basis of an analogy between the liquid crystalline smectic A phase and superconductors [2]. The predicted twist grain boundary (TGB) phase is equivalent to the Abrikosov flux lattice phase of type-II superconductors in an external magnetic field [1, 3]. It consists of twisted smectic A* or smectic C* slabs mediated by grain boundaries of parallel screw dislocations. The first experimental observation of a TGBA* phase was reported by Goodby *et al.* [4, 5]. The first example of the corresponding TGBC* phase was published by Nguyen *et al.* [6].

In this paper we adopt the following nomenclature, which is generally consistent with the proposal outlined in [7]. All liquid crystal phases consisting of chiral molecules are denoted with an asterisk (*), regardless of any possible macroscopic helical superstructure. Therefore the SmA* phase denotes the normal non-helical smectic A phase consisting of chiral molecules. TGBA* refers to the helical version of the SmA* phase, TGBC* to its tilted counterpart and SmC* to the ordinary helielectric tilted chiral smectic phase, exhibiting its intrinsic helical structure [8] as well as the surface stabilized geometry [9].

The model of the TGBA* phase [1] predicts regularly spaced twist grain boundaries consisting of parallel screw dislocations. These are rotated by an angle with respect to those of adjacent grain boundaries. The so formed smectic grains exhibit locally a SmA* layer structure, figure 1 (*c*). Freeze–fracture transmission electron microscopy (TEM) confirms this TGBA* structure [10]. The helical axis of the TGBA* phase is parallel to the smectic layer planes, while the local molecular director of individual smectic slabs rotates discontinuously around the twist axis. A schematic illustration of the structure of the TGBA* phase is given in figure 1. The TGBA* phase exhibits three basic key features: (i) a layered structure; (ii) a helical superstructure; (iii) a helical axis parallel to smectic layer planes. The helical axis is thus perpendicular to the director, a feature which it shares with the helical axis in a cholesteric phase.

The basic structural parameters of the TGBA* phase are the following quantities: l the smectic layer thickness, P the helical pitch, l_b the thickness of the smectic blocks (distance between grain boundaries), l_d the distance between dislocation lines within a grain boundary and $\Delta\alpha$ the twist between consecutive grain blocks (figure 1).

*Author for correspondence.

Journal of Liquid Crystals ISSN 0267-8292 print/ISSN 1366-5855 online
http://www.tandf.co.uk/JNLS/lct.htm
http://www.taylorandfrancis.com/JNLS/lct.htm

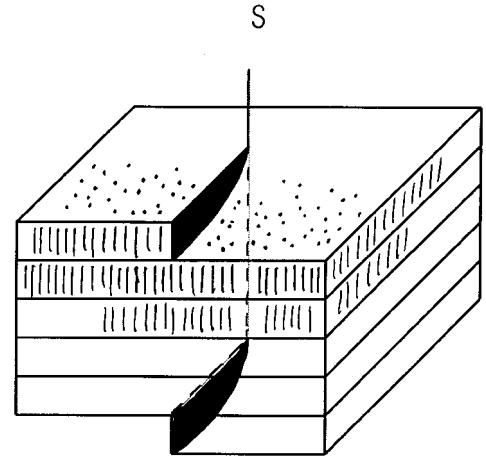

(*a*)

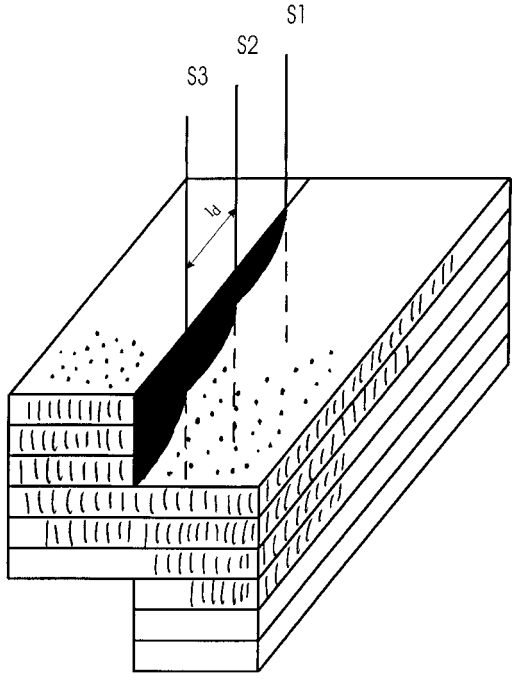

(*b*)

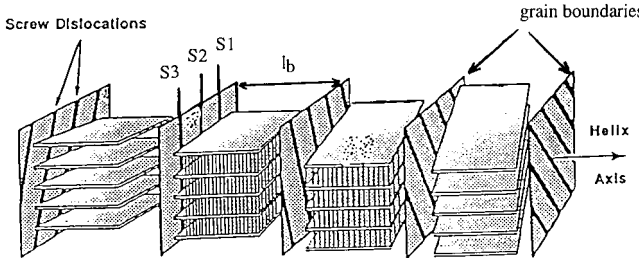

(*c*)

Figure 1. (*a*) Schematic illustration of the smectic layer structure around a single screw dislocation S generating a discontinuous step in the layer structure. (*b*) A periodic array of equidistance screw dislocations S1, S2, S3 ... generating a discontinuous change $\Delta\alpha$ in layer direction along a grain boundary given by $\tan\Delta\alpha = l/l_d$ where l_d is the distance between dislocations. (*c*) A periodic stacking of successively twisted smectic blocks of length l_b between grain boundaries giving a helical structure of pitch P, corresponding to a 2π rotation of the director, as well as the dislocations (which are along the director) and smectic layers. Right handed screw dislocations give rise to a right handed helix.

These parameters are not independent but related by:

$$\Delta\alpha \approx \frac{l}{l_d} \tag{1}$$

[cf. figure 1 (*b*)] and

$$\Delta\alpha = \frac{2\pi l_b}{P} \tag{2}$$

[cf. figure 1 (*c*)], which give

$$P = 2\pi l_b \frac{l_d}{l}. \tag{3}$$

We may estimate the order of magnitude of the distance between screw dislocations by taking the grain block thickness to be of the order of 1000 Å. This parameter was measured in one case (TGBC*) by Navailles *et al.* [11], who first reported X-ray studies on a commensurate twist grain boundary phase. With a pitch P of about 2 μm (see below), this corresponds to $l_d/l \approx 3$ or about 100 Å for the distance between dislocations. So far, X-ray investigations have confirmed both commensurate and incommensurate TGBC* phases [12], while the TGBA* phase generally seems to be incommensurate [13–15]. Very recently however an example of a commensurate TGBA* phase has been reported [16].

2. Experimental

For the texture studies, several different cell preparation techniques and alignment layer treatments were used. Natural textures were observed between untreated glass plates spaced several micrometres apart. Samples were generally prepared by melting the compound on a glass slide and covering it with a cover slip. Planar oriented samples were obtained by spin-coating the substrates with polyimide and subsequent unidirectional rubbing. This induces a planar anchoring condition which promotes an orientation of the molecular long axis parallel to the substrates. Cell gaps were chosen to be $d = 8$ μm, and wedge cell preparations such that a wedge from

$d = 0$ μm to $d = 12$ μm was formed over a length of 15 mm. Homeotropic orientation was achieved by coating the substrates with lecithin, promoting an orientation of the molecular long axis perpendicular to the substrate plane. Cell gaps were chosen as above. For the comparative study of the textures of a cholesteric twist inversion compound, wedge cells with planar anchoring conditions were produced with a maximum thickness of $d = 100$ μm. Homeotropic wedge cells had a maximum gap of $d = 12$ μm.

The materials used were two compounds of a homologous series of mesogens of the diarylethane α-chloroalkyl ester type shown below [17, 18]:

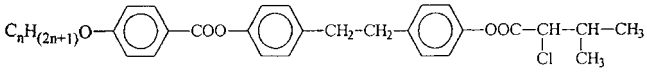

Phase sequences on cooling (D7 and D8 for $n = 7, 8$, respectively) were:

D7: I 133.2 N* 121.1 TGBA* 120.8 SmC* and higher ordered phases,

D8: I 134.5 N* 129.4 TGBA* 129.2 SmA* 125.6 SmC* and higher ordered phases.

The cholesteric twist inversion compound was 4-[(*S*,*S*)-2,3 epoxyhexyloxy]phenyl 4-decyloxybenzoate [19, 20], commercially available from Aldrich and having the structure below:

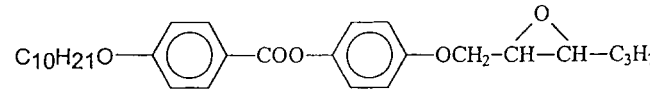

with the phase sequence on cooling:

I 95.7 N* 78.9 TGBA* 78.6 SmC* 57.2 SmI*.

Texture studies were carried out with a Nikon OPTIPHOT2-POL polarizing microscope equipped with a Mettler FP52 hot stage and a Sony Hyper HAD model SSC-DC38P digital video camera in combination with imaging software from Bergström Instruments AB.

3. Experimental results and discussion

3.1. *General textures*

Generally the phase stability range of twist grain boundary phases is rather small, resulting in only a narrow temperature interval of approximately 1 K where these phases may be observed. The phase sequence in which the TGBA* phase is incorporated can vary, but often the TGBA* phase is located between the cholesteric high temperature phase and the SmA* low temperature phase. If the temperature interval of phase existence becomes very small, in the order of a few tenths of

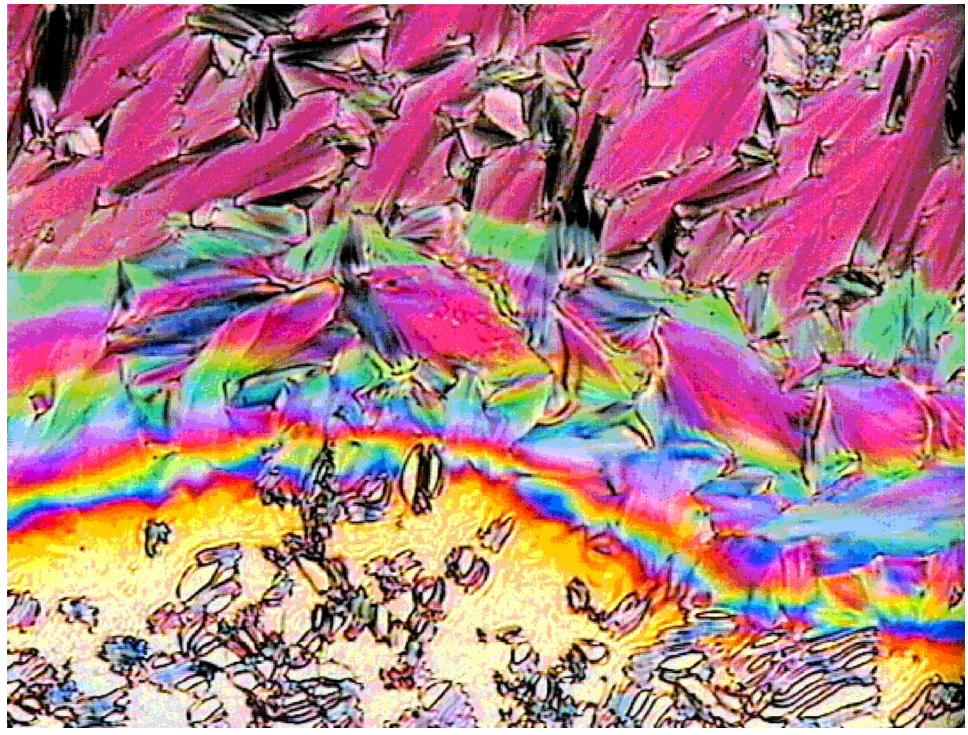

Figure 2. Sample of D8 prepared under a temperature gradient from top to bottom, exhibiting in that direction the SmA* fan-shaped texture, the TGBA* phase and the cholesteric oily-streak texture, respectively. The phase boundaries are clearly visible, allowing observation of the TGBA* phase even for a narrow temperature interval.

Kelvins, the temperature gradient method can be useful to identify the occurrence of TGBA*. An example is depicted in figure 2 for compound D8, with a temperature gradient from top to bottom, showing the sequence SmA*–TGBA*–N*. Phase boundaries between SmA* and TGBA* as well as between TGBA* and N* are clearly

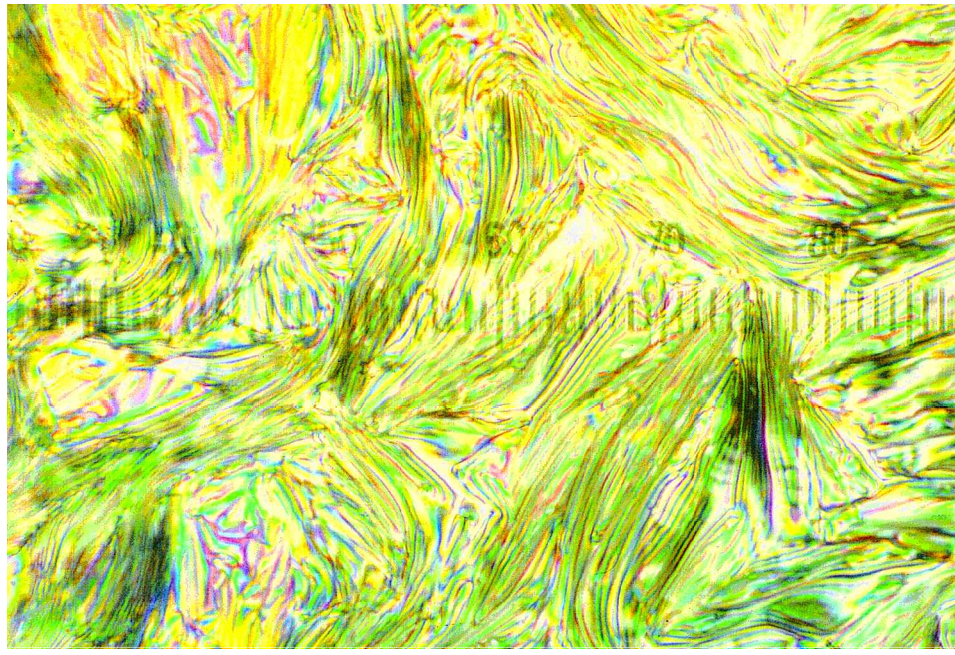

Figure 3. Natural texture of the TGBA* phase of D8 prepared between untreated glass plates.

Figure 4. Texture of the TGBA* phase in a cell of gap $d = 8\ \mu m$ with planar boundary conditions. The molecular long axes are oriented in the plane of the substrate, and the helix axis is perpendicular to the bounding glass plates. The photograph was taken on cooling the sample; different colours correspond to different twist states due to hysteresis effects and a non-uniform temperature distribution.

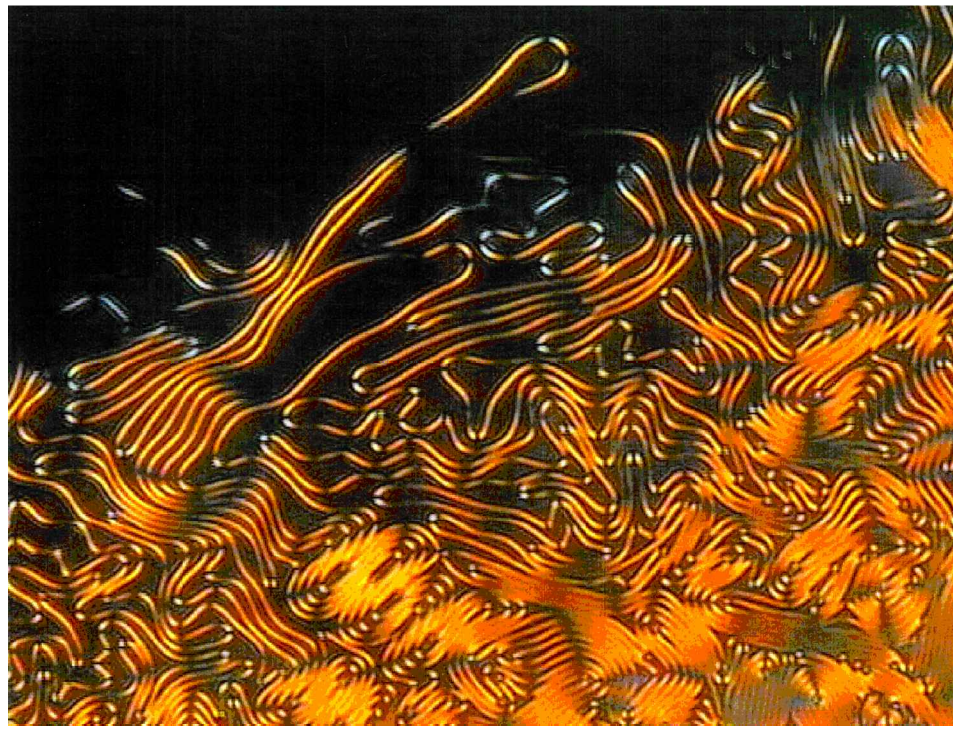

Figure 5. Filament texture of the TGBA* phase of D8 at the transition to SmA* (black region, upper left). Homeotropic boundary conditions induce a fingerprint-like, filament texture, while in the non-helical SmA* phase the director is oriented along the direction of light propagation, thus appearing dark. From the distance between the helix lines, the TGBA* pitch can be estimated.

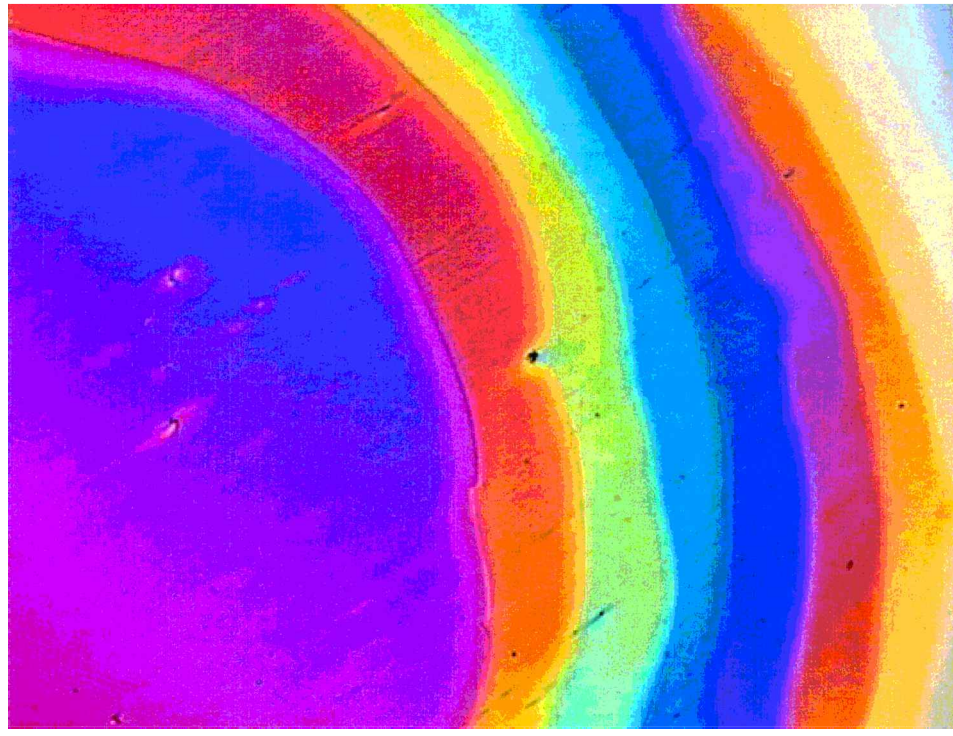

Figure 6. Wedge cell preparation of the D8 TGBA* phase with planar boundary conditions. The observed Grandjean-like steps correspond to twist states varying by half the pitch. Due to a slight temperature gradient, the SmA* phase is exhibited at the left side of the photograph, appearing coloured, because the director is oriented obliquely relative to the polarizers.

visible. The range of the twist grain boundary phase in this case is approximately 0.2 K. A natural texture of the TGBA* phase of D8 prepared between untreated glass plates is shown in figure 3.

Subjecting the TGBA* phase to planar or pseudo-planar (with a small pretilt) boundary conditions, results in an orientation of the molecular long axis approximately parallel to the substrate plane, thus the helical axis is oriented essentially perpendicular to the glass substrate. This leads to a texture very similar to one observed for a cholesteric phase, known as the Grandjean texture [21, 5]. The example for D8 in an

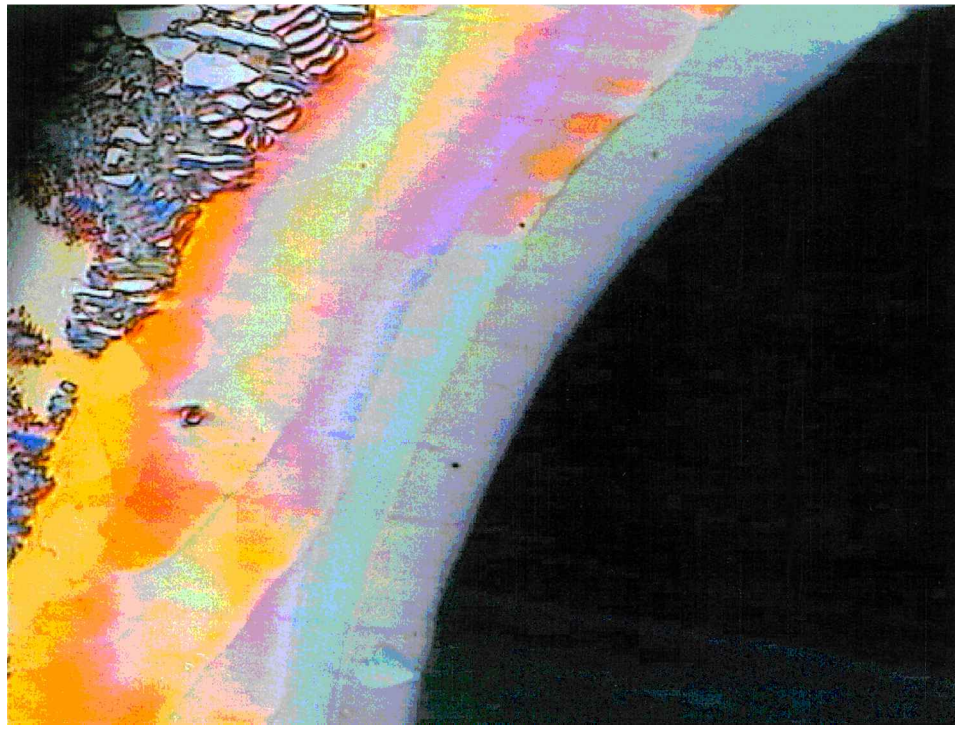

(*a*)

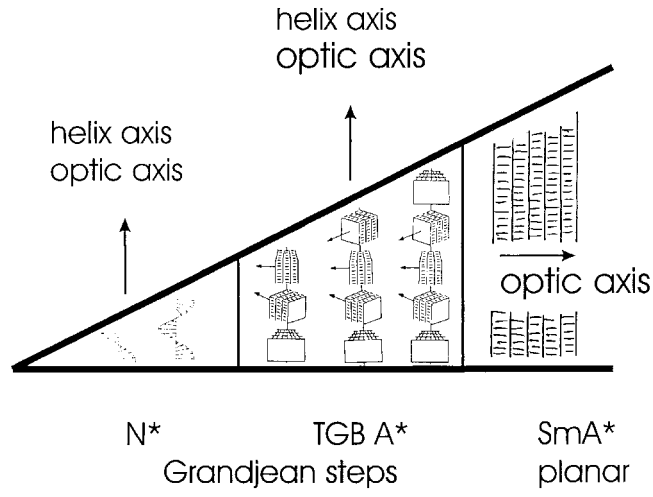

(*b*)

Figure 7. (*a*) Texture of D8 under a temperature gradient with the sample prepared in a wedge with planar boundary conditions. On the lower right hand side, the SmA* is oriented with the director parallel to one of the polarizer directions, thus appearing dark. In the centre part, the TGBA* phase appears with Grandjean lines due to its helical structure (twist axis perpendicular to the substrate plane, along the direction of light propagation). On the top left the transition to the cholesteric phase with its typical oily-streaks texture can be observed. (*b*) Schematic illustration of the director and smectic layer configurations observed in the corresponding texture photograph, figure 7 (*a*).

8 μm cell, found in figure 4, shows the TGBA* phase obtained on cooling under planar anchoring conditions and with different twist states, corresponding to the different colours observed. Preparations of the TGBA* phase under homeotropic boundary conditions exhibit textures very similar to the so-called 'fingerprint' texture observed for cholesterics. Figure 5 shows D8 at the transition from SmA*, which adopts a homeotropic director configuration and thus appears black. The yellow filaments of the TGBA* phase are rather characteristic, but may also be mistaken for a cholesteric texture. This will be discussed in more detail below, when wedge cells

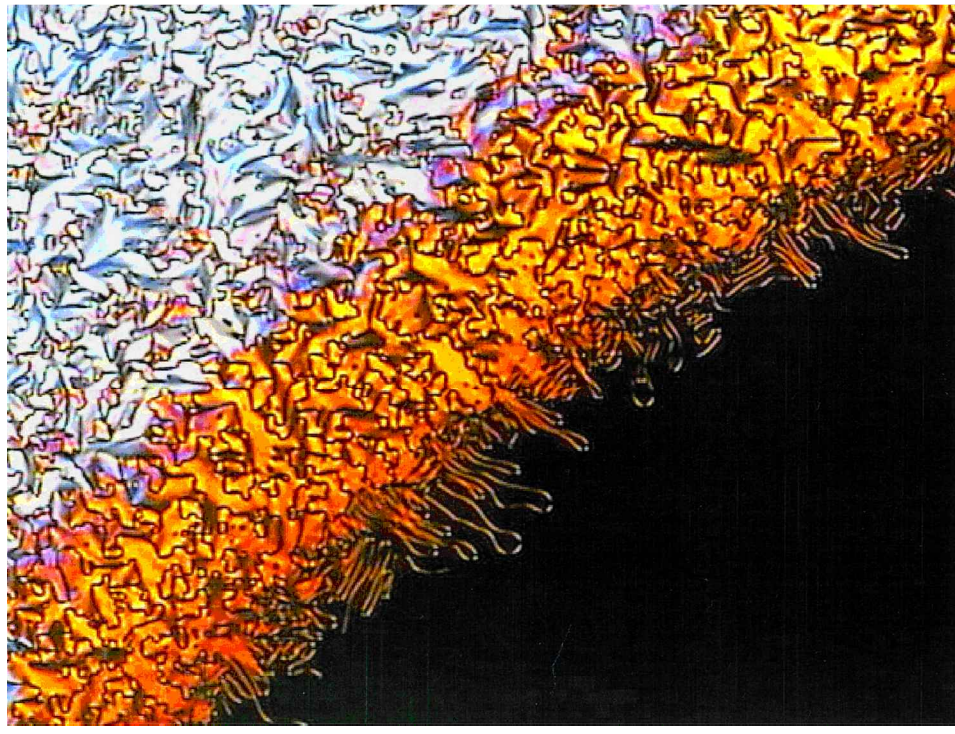

(*a*)

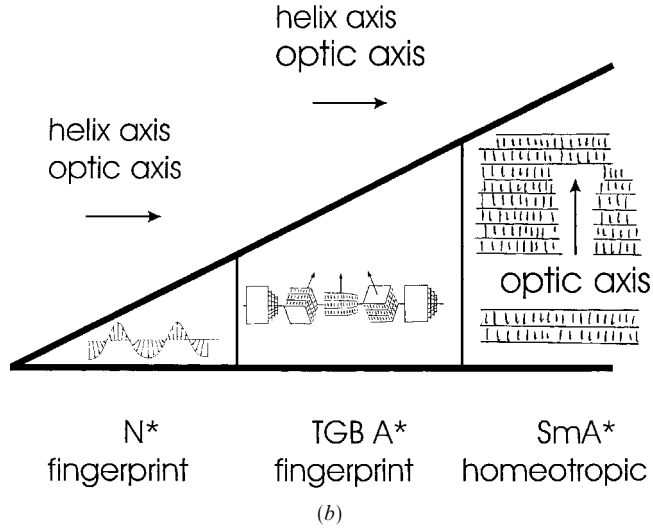

(*b*)

Figure 8. (*a*) Texture of D8 in a wedge cell with homeotropic boundary conditions under a temperature gradient. The dark area (bottom right) corresponds to the SmA* phase with the director oriented parallel to the direction of light propagation. In the middle part the TGBA* filament texture is observed, clearly separated from the cholesteric texture as can be seen by a change in birefringence (upper left). (*b*) Schematic illustration of the director and smectic layer configurations in the corresponding texture photograph, figure 8 (*a*).

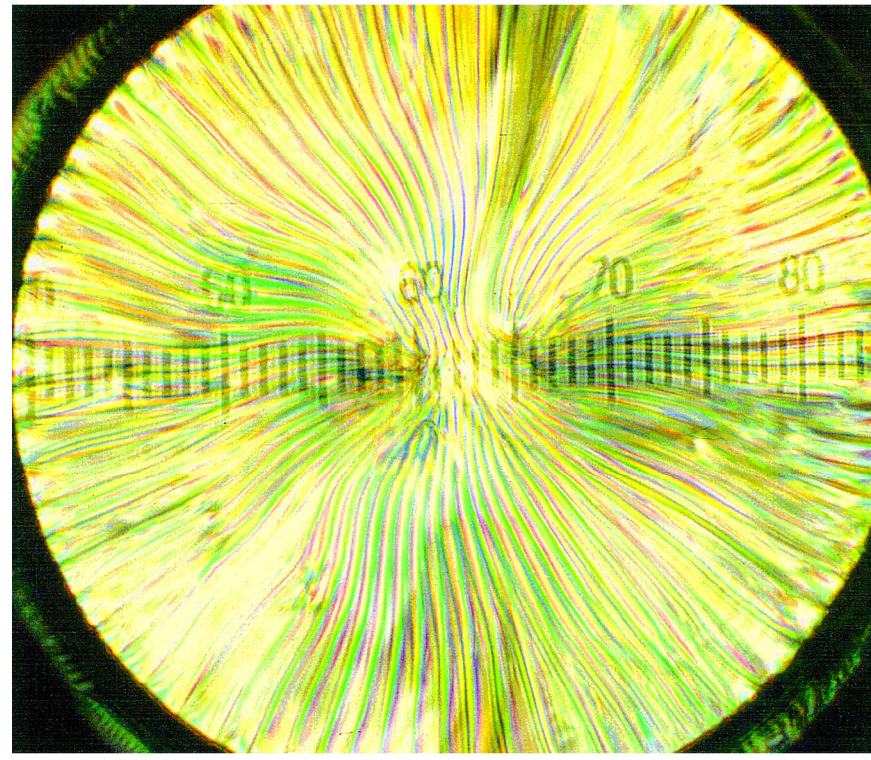

(*a*)

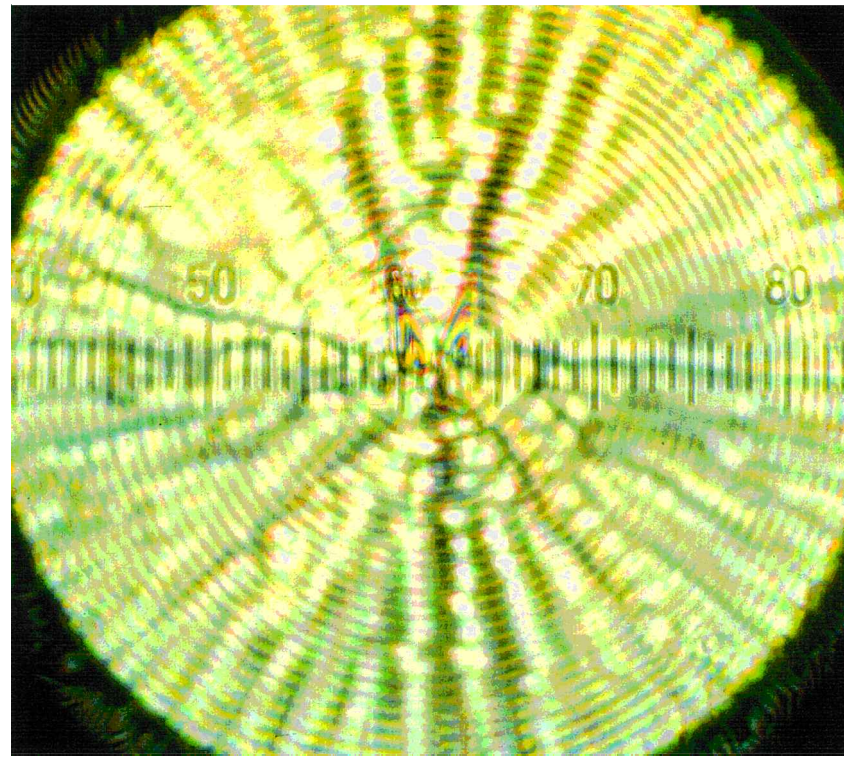

(*b*)

Figure 9. (*a*) Droplet preparation of the TGBA* phase of D7 exhibiting a radial arrangement of defect lines (pitch lines). The helix axis is parallel to the smectic layers which are concentric. (*b*) The defect structure of the SmC* phase in the same droplet preparation. Pitch lines are parallel to the smectic layers, and the helix axis is oriented perpendicular to the smectic layer planes. This comparison demonstrates that the smectic layers within the droplet are oriented in the same way for both TGBA* and SmC*, while the direction of the helical axis is turned by 90°, from parallel to perpendicular to the smectic layers, respectively.

are considered. The filament texture was first reported as a characteristic texture in the original article on the experimental discovery of the TGBA* phase [4, 5] for free-standing films. The structure of the filaments was discussed in a preliminary way in [22] and in much more detail by Gilli and Kamaye [23]. As in cholesterics, the helix axis lies in the plane of the substrate and the equidistant line pattern allows an estimation of the pitch, which in this case is approximately $P = 2$–$3\ \mu m$ in regions not too close to the TGBA*–SmA* transition.

3.2. *Wedge cell preparations*

Preparation of the TGBA* phase in a wedge cell with planar boundary conditions orients the molecular long axis parallel to the substrate and the helical axis perpendicular to it. Thus we observe a Grandjean-like texture with steps between twist states varying by half the pitch [21, 24–26] as illustrated in figure 6 for D8. On the left side of the photograph the uniformly oriented SmA* phase is observed, with the director oriented at an angle with respect to both of the polarizer directions (thus appearing coloured). Only in very few cases have the slab dislocations due to single grain boundaries also been observed, in addition to the Grandjean steps, as a superimposed line pattern for wedge cell preparation [25]. Apparently their observation is easier for the TGBC* phase than for TGBA* (compare texture photographs of figures 4 and 6 of ref. [25]).

In figure 7 (*a*) we see again a planar wedge cell preparation of D8, this time under a more pronounced temperature gradient from left to right. The right part of the texture shows the SmA* phase with its optical axis (the long molecular axis) parallel to one of the polarizer directions, thus appearing black. In the middle part we observe the Grandjean-like steps of the TGBA* phase for different twist states with the helix axis parallel to the direction of light propagation, before a typical cholesteric texture with oily-streaks is observed at the higher temperatures on the left. Figure 7 (*b*) schematically illustrates the director configuration and direction of the helix axis for the different phases corresponding to figure 7 (*a*).

In comparison we can look at a wedge cell of D8 prepared with homeotropic boundary conditions, thus promoting an orientation of the molecular long axis perpendicular to the substrate plane. In figure 8 (*a*), the sample is again observed under a temperature gradient from left to right. The black area represents the SmA* phase, this time in a homeotropic orientation. The filament texture of the TGBA* phase is observed in the middle part of the photograph, changing into a cholesteric fan-like texture at higher temperatures to the left. The phase boundary between the TGBA* and cholesteric (N*) phases can clearly be observed by a discontinuous change in birefringence. Figure 8 (*b*) depicts the director and smectic layer configuration related to the situation illustrated by the respective textures in figure 8 (*a*).

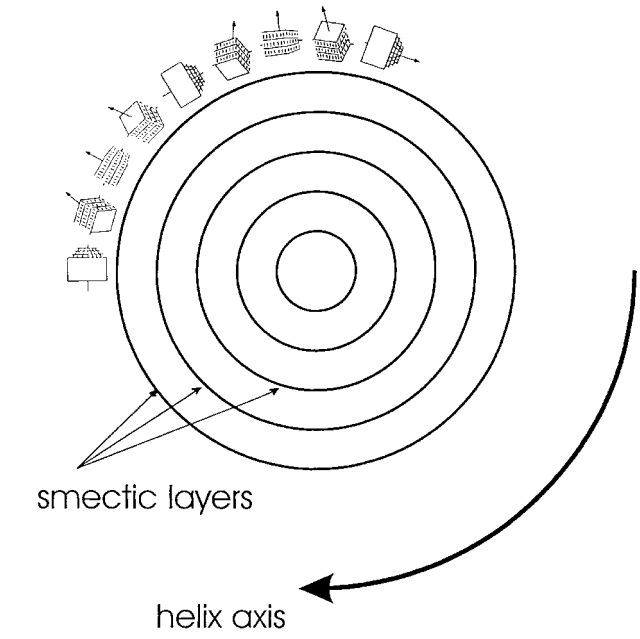

(*a*)

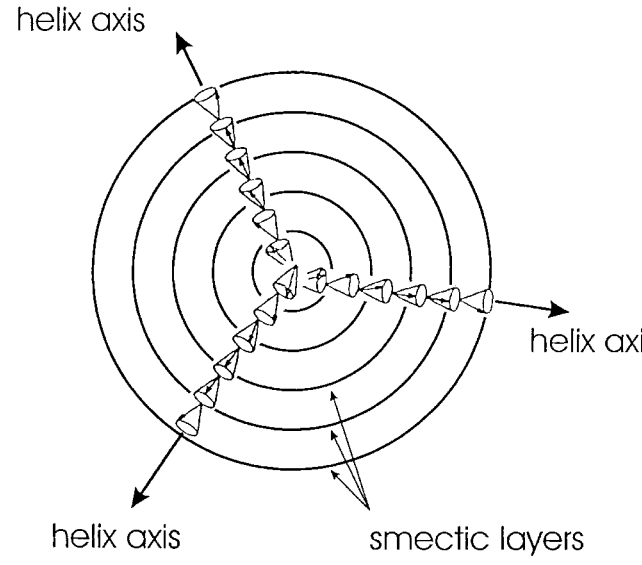

(b)

Figure 10. Schematic illustration of the smectic layer structure, helix direction and director configuration corresponding to figure 9. (*a*) TGBA* droplet and (*b*) SmC* droplet.

3.3. *Droplet preparations*

Considering the differences in smectic structure and director configuration between the TGBA* and the SmC* phase, it is clear that for the former the direction of the helix axis is along the smectic layer planes, while for the latter the helix axis is oriented perpendicular to the smectic layer planes. This feature can be directly verified by texture observation on droplets prepared between a glass slide and a cover slip with basically planar anchoring conditions. In the TGBA* phase, the helical axis is oriented along the smectic layers, and so the disclination lines ('pitch lines'), formed perpendicular to the helix axis, give rise to a radial line pattern as observed for D7 in figure 9 (*a*). On lowering the temperature into the SmC* phase, a change of the disclination line pattern is observed. The smectic layers are still oriented in a concentric fashion, but now the twist axis is directed along the smectic layer normal, and the disclination lines are now observed parallel to the smectic layers, reflecting their concentric arrangement, as illustrated in figure 9 (*b*). The respective photographs are taken from earlier investigations on D7, reported in [17]. Figures 10 (*a*) and 10 (*b*) depict the corresponding smectic layer and director configuration.

3.4. *Preparations in thin cells*

If a twist grain boundary phase is confined to sufficiently thin cells, its helical superstructure may be unwound. In our investigations on planar and homeotropic wedge cells we observed the following behaviour: with planar boundary conditions, the TGBA* helix is unwound when the cell gap reaches dimensions of approximately twice the TGBA* pitch, in our case about 4 μm. This value is smaller than that reported in another study

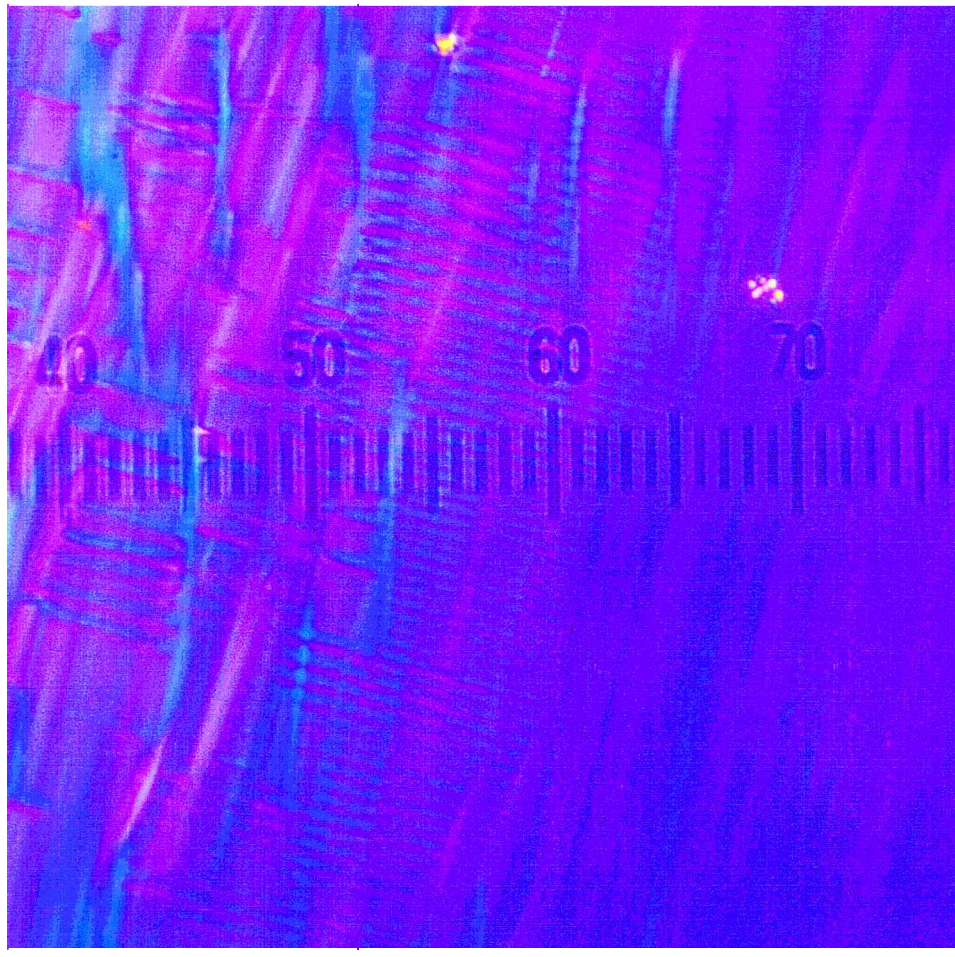

Figure 11. Preparation of D7 in a thin cell of gap $d = 4\ \mu m$ with monostable planar boundary conditions. The helical structure of the TGBA* phase is unwound, thus unifying the structures of the constituent grains forming the TGBA* phase. This structure is of the SmA* type as seen in the right hand side of the photograph, exhibiting a well oriented SmA* texture. To the left we observe the transition to the SmC* phase accompanied by partial helix lines. It is emphasised that in thick cells D7 does *not* exhibit a SmA* phase, so that in this figure we actually observe the effect of TGBA* helix unwinding by the surface in a thin cell, so creating a SmA* phase.

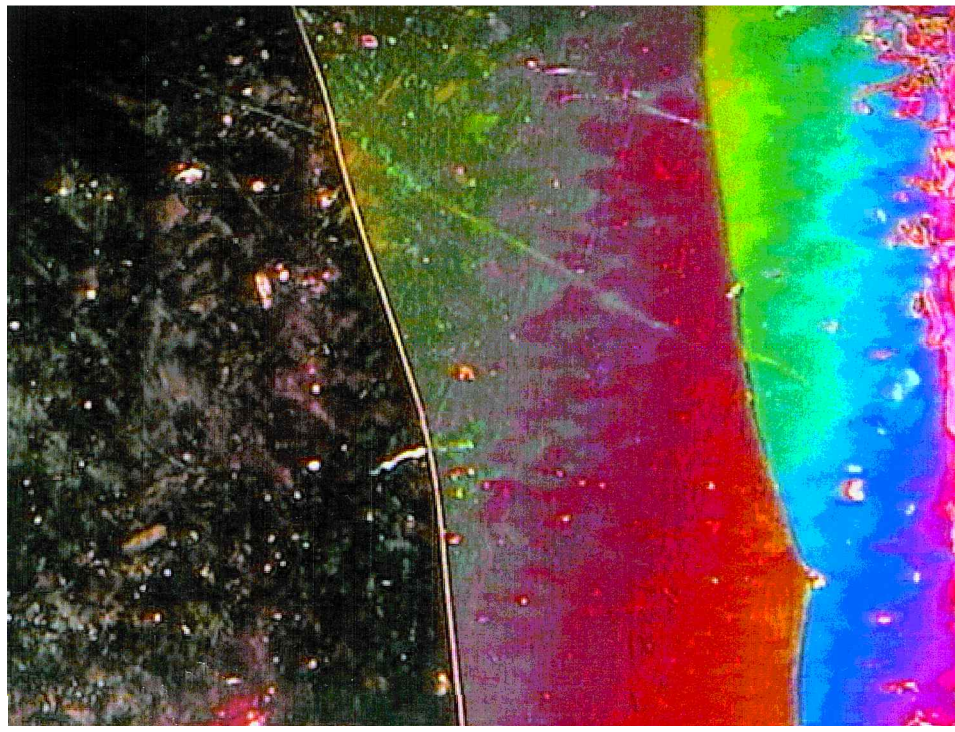

Figure 12. A cholesteric phase at a helix inversion point in a wedge cell treated for planar alignment. The dark part of the texture on the left hand side exhibits the untwisted nematic state with the director parallel to one of the polarizer directions, similarly to the SmA* phase in figure 7 (*a*). The twisted cholesteric state exhibits Grandjean steps as does the TGBA* phase, figure 7 (*a*).

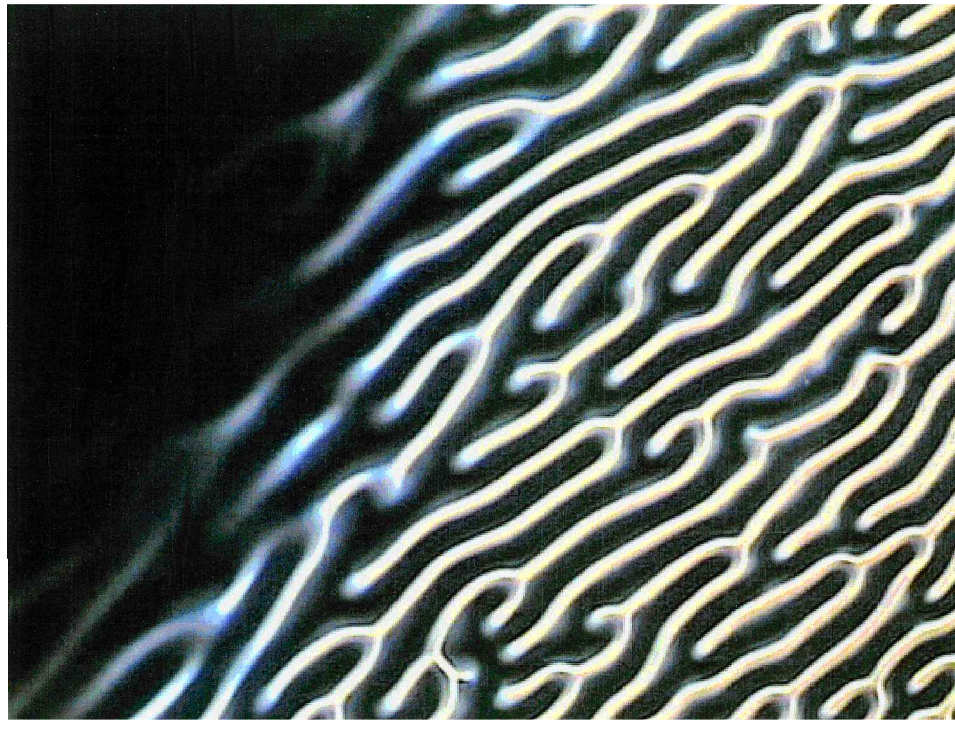

Figure 13. Texture of a cholesteric phase in the vicinity of a twist inversion point under homeotropic boundary conditions. The dark part of the photograph exhibits the unwound, non-helical state with the director parallel to the direction of light propagation, resembling the behaviour observed for the SmA* phase in figure 8 (*a*). On the right hand side the fingerprint-like cholesteric texture is somewhat similar to the filaments observed for the TGBA* phase in homeotropic cells.

[27, 28] and may be caused by a difference in anchoring strength. We did not observe a similar behaviour for homeotropic wedge cells. In this case the filament texture was still observed for quite thin cell gaps of about 2 μm.

From textures of samples with an unwound helix, we can deduce the actual structure within the TGB grains. Figure 11 clearly reveals that the TGBA* building blocks are of the Smectic A* type. The compound used here was D7, which does not exhibit a SmA* phase, but simply shows a phase sequence (on cooling) given by I–N*–TGBA*–SmC* and higher ordered phases. Figure 11 was taken using a 4 μm cell with monostable planar boundary conditions and a slight temperature gradient from left to right. The left part clearly shows the SmC* phase accompanied by the occurrence of some disclination lines ('pitch lines') due to the helix axis perpendicular to the smectic layers and in the plane of the substrate. At the right side of the photograph, on the high temperature side, a well oriented texture of a SmA* phase is observed. Its uniform direction of the optic axis (corresponding to the smectic layer normal) is lying in the plane of the cell. This part of the sample can therefore be brought into extinction, which rules out any question that it is a cholesteric phase in the Grandjean orientation.

3.5. *Comparison with cholesteric textures at a twist inversion point*

Under certain conditions, the textures of a cholesteric phase in the vicinity of a twist inversion point may look similar to that of a TGBA* phase. Figure 12 shows the cholesteric phase of the epoxy compound in the vicinity of the twist inversion, prepared in a wedge cell with planar boundary conditions. The left part of the figure exhibits the untwisted state with the nematic director oriented parallel to the substrate plane along one of the polarizer directions, resembling the SmA* phase of figure 7 (*a*). In the right part we observe the cholesteric Grandjean steps due to the helical structure with twist axis perpendicular to the substrate plane, resembling the TGBA* phase of figure 7 (*a*).

Figure 13 shows the corresponding situation for homeotropic boundary conditions. The black part on the left side shows the untwisted nematic state with the director oriented along the direction of light propagation, resembling the SmA* phase of figure 8 (*a*). The pseudo-helical cholesteric structure on the right appears somewhat similar to the filaments of the TGBA* phase of figures 5 and 8 (*a*).

4. Summary

We have given a review of textures of the TGBA* phase for several different geometries and surface treatments and explained their appearance, considering the key features of the TGB structure: a helical superstructure, smectic layers and a helix axis along the smectic layer plane. Textures observed for the TGBA* phase are generally more similar to those of a cholesteric than to those of a SmA* phase. Monostable planar boundary conditions lead to Grandjean-like textures, while for homeotropic cells filaments similar to a fingerprint pattern are observed. Narrow TGBA* phases can be detected by observation of samples under a temperature gradient. For thin cells with planar anchoring, the helical structure of the TGBA* phase can be unwound and the untwisted SmA* structure of the constituent grains is revealed.

The authors would like to acknowledge the financial support of the Alexander von Humboldt-Stiftung through a Feodor-Lynen fellowship (I.D.), as well as basic support from the Swedish Foundation for Strategic Research.

References

[1] Renn, S. R., and Lubensky, T. C., 1988, *Phys. Rev. A*, **38**, 2132.
[2] De Gennes, P. G., 1972, *Solid State Comm.*, **10**, 753.
[3] Renn, S. R., and Lubensky, T. C., 1991, *Mol. Cryst. liq. Cryst.*, **209**, 349.
[4] Goodby, J. W., Waugh, M. A., Stein, S. M., Chin, E., Pindak, R., and Patel, J. S., 1989, *Nature*, **337**, 449.
[5] Goodby, J. W., Waugh, M. A., Stein, S. M., Chin, E., Pindak, R., and Patel, J. S., 1989, *J. Am. chem. Soc.*, **111**, 8119.
[6] Nguyen, H. T., Bouchta, A., Navailles, L., Barois, P., Isaert, N., Twieg, R. J., Maroufi, A., and Destrade, C., 1992, *J. Phys. II Fr.*, **2**, 1889.
[7] Lagerwall, S. T., 1988, *Ferroelectrics*, **85**, 497.
[8] Martinot-Lagarde, Ph., 1976, *J. de Phys.*, **37**, C3-129.
[9] Clark, N. A., and Lagerwall, S. T., 1980, *Appl. Phys. Lett.*, **36**, 899.
[10] Ihn, K. J., Zasadzinski, J. A. N., Pindak, R., Slaney, A. J., and Goodby, J., 1992, *Science*, **258**, 275.
[11] Navailles, L., Barois, P., and Nguyen, H. T., 1993, *Phys. Rev. Lett.*, **71**, 545.
[12] Navailles, L., Pindak, R., Barois, P., and Nguyen, H. T., 1995, *Phys. Rev. Lett.*, **74**, 5224.
[13] Srajer, G., Pindak, R., Waugh, M. A., and Goodby, J. W., 1990, *Phys. Rev. Lett.*, **64**, 1545.
[14] Hardouin, F., Achard, M. F., Jin, J.-I., Shin, J.-W., and Yun, Y.-K., 1994, *J. de Phys. II Fr.*, **4**, 627.
[15] Galerne, Y., 1994, *J. de Phys. II Fr.*, **4**, 1699.
[16] Navailles, L. *et al.*, 1998, presentation at the workshop: Ten years of the Twist-Grain-Boundary Phase, Philadelphia, April 1998.
[17] Dierking, I., Gießelmann, F., and Zugenmaier, P., 1994, *Liq. Cryst.*, **17**, 17.
[18] Dierking, I., Gießelmann, F., Kußerow, J., and Zugenmaier, P., 1994, *Liq. Cryst.*, **17**, 243.
[19] Walba, D. M., Vohra, R. T., Clark, N. A., Handschy, M. A., Xue, J., Parma, D. S., Lagerwall, S. T., and Skarp, K., 1986, *J. Am. chem. Soc.*, **108**, 7424.

[20] DIERKING, I., GIEßELMANN, F., ZUGENMAIER, P., KUCZYNSKI, W., LAGERWALL, S. T., and STEBLER, B., 1993, *Liq. Cryst.*, **13**, 45.
[21] GRANDJEAN, M. F., 1921, *C.R. Acad. Sci.*, **172**, 71.
[22] SLANEY, A. J., and GOODBY, J. W., 1991, *J. mater. Chem.*, **1**, 5.
[23] GILLI, J. M., and KAMAYE, M., 1992, *Liq. Cryst.*, **12**, 545.
[24] CANO, R., 1968, *Bull. Soc. Fr. Mineral. Cristallogr.*, **91**, 20.
[25] ISAERT, N., NAVAILLES, L., BAROIS, P., and NGUYEN, H. T., 1994, *J. Phys. II Fr.*, **4**, 1501.
[26] NAVAILLES, L., NGUYEN, H. T., BAROIS, P., ISAERT, N., and DELORD, P., 1996, *Liq. Cryst.*, **20**, 653.
[27] KUCZYNSKI, W., and STEGEMEYER, H., 1994, *Ber. Bunsenges. phys. Chem.*, **98**, 1322.
[28] KUCZYNSKI, W., and STEGEMEYER, H., 1995, *Mol. Cryst. liq. Cryst.*, **260**, 377.